AIP Advances

Temperature dependence of the electrical resistivity of LaxLu1-xAs

S. Rahimi, E. M. Krivoy, J. Lee, M. E. Michael, S. R. Bank, and D. Akinwande

Citation: AIP Advances **3**, 082102 (2013); doi: 10.1063/1.4817830
View online: http://dx.doi.org/10.1063/1.4817830
View Table of Contents: http://scitation.aip.org/content/aip/journal/adva/3/8?ver=pdfcov
Published by the AIP Publishing

Temperature dependence of the electrical resistivity of $La_xLu_{1-x}As$

S. Rahimi,[1] E. M. Krivoy,[1] J. Lee,[1] M. E. Michael,[2] S. R. Bank,[1] and D. Akinwande[1]

[1]*Microelectronics Research Center, The University of Texas at Austin, Austin, Texas 78712, USA*

[2]*Department of Mechanical Engineering, University of Virginia, Charlottesville, Virginia 22904, USA*

(Received 11 June 2013; accepted 23 July 2013; published online 1 August 2013)

We investigate the temperature-dependent resistivity of single-crystalline films of $La_xLu_{1-x}As$ over the 5–300 K range. The resistivity was separated into lattice, carrier and impurity scattering regions. The effect of impurity scattering is significant below 20 K, while carrier scattering dominates at 20–80 K and lattice scattering dominates above 80 K. All scattering regions show strong dependence on the La content of the films. While the resistivity of 600 nm LuAs films agree well with the reported bulk resistivity values, 3 nm films possessed significantly higher resistivity, suggesting that interfacial roughness significantly impacts the scattering of carriers at the nanoscale limit. [http://dx.doi.org/10.1063/1.4817830]

The rare-earth monopnictides (RE-V) with rocksalt structures have been the focus of experimental and theoretical studies in the past few decades.[1–14] The RE compounds are especially interesting because their lattice constants are compatible with a variety of III-V substrates, allowing for the growth of high-quality single crystalline material by molecular beam epitaxy (MBE).

Studies on the energy band structures of a number of RE-As compounds such as ErAs, GdAs, ScAs, TmAs, YbAs, YAs, LuAs and LaAs suggest a semimetallic character with a slight overlap between the valance and conduction energy bands.[3–7,14] Moreover, the temperature-dependent magnetoresistance measurements of ErAs, a well-studied compound from the RE-As group, shows a semimetallic character for ErAs with a relatively low density of electrons and holes, ~2–4 $\times$ 10^{20} cm^{-3} extracted at 1.4 K.[4] Further studies on the charge transport properties and the energy band diagrams of some of the RE-As alloys such as $Sc_xEr_{1-x}As$, suggest that the semimetallic character of the binaries is preserved in the ternary alloys.[8,9] This combination of semimetallic properties and the state-of-the-art crystal and film growth on III-V substrates, in addition to the potential of fabricating novel quantum-well systems based on semimetal-semiconductor heterostructures, has given rise to various applications including transparent contacts for optical applications,[10] non-linear terahertz electronics and resonant tunneling hot electron transistors,[11,12] and plasmonic structures.[13]

While several theoretical studies on the electrical properties and energy band diagrams of LaAs and LuAs, the two end-points of the lanthanide series of the RE-As, have been reported previously,[7,14,23] the experimental electrical properties of these compounds remain largely unexplored. We previously reported the temperature-dependence resistivity of LuAs and LaAs films at 77–300 K temperature range.[15,16] Here we report the studies of the temperature-dependent electrical resistivity of these two compounds at 5–300 K range. We also investigated the effect of La concentration and the film thickness on the resistivity of $La_xLu_{1-x}As$ ternary alloy films. The charge scattering mechanisms are discussed and the impact of lanthanum content on the electrical resistivity of $La_xLu_{1-x}As$ films is reported.

The MBE growth of LuAs on GaAs substrates was first reported by Palmstrøm et al.[2] In the same report, the electrical resistivity of 65 Å of LuAs grown on GaAs was reported at room

temperature and at 1.5 K with no reports on the temperature-dependent variation of the resistivity. A semimetallic character was established for LuAs through energy band structure calculations.[7] Studies of the energy band diagram of LaAs suggest a semimetallic character with a low density of carriers at the Fermi level.[14] However, the charge transport properties of LaAs have not been investigated experimentally so far, likely due to significant growth challenges that must first be overcome in growing LaAs epitaxially on III-V materials. In our prior work, we reported a new technique involving the growth of high-quality epitaxial LaAs utilizing a thin LuAs barrier layer to prevent interfacial instability between the LaAs and III-V layers.[15] Thick films (500–600 nm) of LaAs, LuAs and $La_xLu_{1-x}As$ (x = 48%), as well as thin films (10 ML or ~3 nm) of LuAs and $La_xLu_{1-x}As$ (x = 5, 9 and 15%) were grown for the current study.

Samples were grown by solid-source molecular beam epitaxy (MBE) in an EPI Mod. Gen. II system at 460 °C with an As:RE beam equivalent pressure ratio of 46:1. The 10 ML samples consist of semi-insulating (100) GaAs substrates with a 200 nm GaAs buffer, followed by 10 ML of LuAs or $La_xLu_{1-x}As$ (x = 5, 9 and 15 %) and a 15 nm GaAs capping layer. It was found that for $La_xLu_{1-x}As$ alloy films with La content less than 15%, thin LuAs barriers were unnecessary and the low concentration of La in the films did not indicate poor morphology in the observed in-situ RHEED patterns or ex-situ XRD scans. Film thickness was determined in-situ by reflection high-energy electron diffraction (RHEED) oscillations and confirmed ex-situ by X-ray diffraction (XRD) and cross-sectional transmission electron microscopy (XTEM).[15,16] Thick samples consisting of 600 nm of LuAs, 500 nm of LaAs and 500 nm of $La_{0.48}Lu_{0.52}As$ were also investigated. The growth of thicker films is similar to the growth of thin 10 ML films, with the main difference being the integration of 10 ML top and bottom LuAs spacer layers surrounding the LaAs and $La_{0.48}Lu_{0.52}As$ films to prevent interfacial instability. The details of the growth of thick $La_xLu_{1-x}As$ alloys will be presented elsewhere.[17]

The resistivity measurement method used for this study employs cross sheet Van der Pauw (VDP) resistor structures.[18] Figure 1(a) illustrates the fabrication steps taken in order to make the VDP structures. After the initial cleaning steps, the samples were coated with negative resist AZ-5214 followed by photolithography to define Ni (10 nm) and Au (40 nm) electrodes, which were deposited by electron-beam evaporation. The electrodes were then annealed at 260 °C in an N_2 ambient in order to form diffused Ohmic contacts to the buried LuAs, $La_xLu_{1-x}As$, and LaAs films.[12] In the second photolithography step, device isolation was achieved by wet etching of the GaAs capping layer, the LuAs/$La_xLu_{1-x}As$/LaAs films and the GaAs buffer layer using a solution of H_2O:H_3PO_4:H_2O_2 with 20:1:1 composition. Figure 1(b) shows the VDP structures fabricated on a 10 ML LuAs sample.

In Figure 2(a), we present the electrical resistivity measurements of thin (10 ML) and thick (600 nm) LuAs films over the 5–300 K range. The residual resistivity ratios of the 600 nm and 10 ML films, which is defined as the ratio of resistivity at 300 K to the constant resistivity value at 5 K, are 2.96 and 1.49 respectively. These values demonstrate small residual resistivity and high quality of these single-crystalline samples. The resistivity values at 5 K and 300 K are quantitatively consistent with those reported earlier.[2] At low temperatures (below 20 K), the resistivity of both samples is constant with temperature, consistent with the temperature-independent elastic scattering of carriers by impurities. As we shall discuss more in the analysis to follow, the difference between the residual resistivity of 600 nm and 10 ML LuAs films below 20 K could be largely due to the pronounced interfacial roughness scattering of carriers in the 10 ML film. While the 10 ML LuAs is more strained to the GaAs lattice than 600 nm film, this additional strain impact the lattice constant of 10 ML films only slightly compared to the bulk phase (600 nm thick films) and thus does not have a significant effect on the residual resistivity of the 10 ML films.[16]

Figure 2(b) shows the electrical resistivity of 10 ML (3 nm) $La_xLu_{1-x}As$ with x = 0, 5, 9 and 15% La concentration. At 5 K, the residual resistivity is observable similar to the pure LuAs films and varies from ~ 60 $\mu\Omega$-cm for LuAs to ~200 $\mu\Omega$-cm for $La_xLu_{1-x}As$ (x = 15%). This increase in the residual resistivity (ρ_o) of alloy films is consistent with the following equation for residual resistivity of metals:[19]

$$\rho_o = \frac{m v_d}{n e^2} \frac{x_i}{a} \quad (1)$$

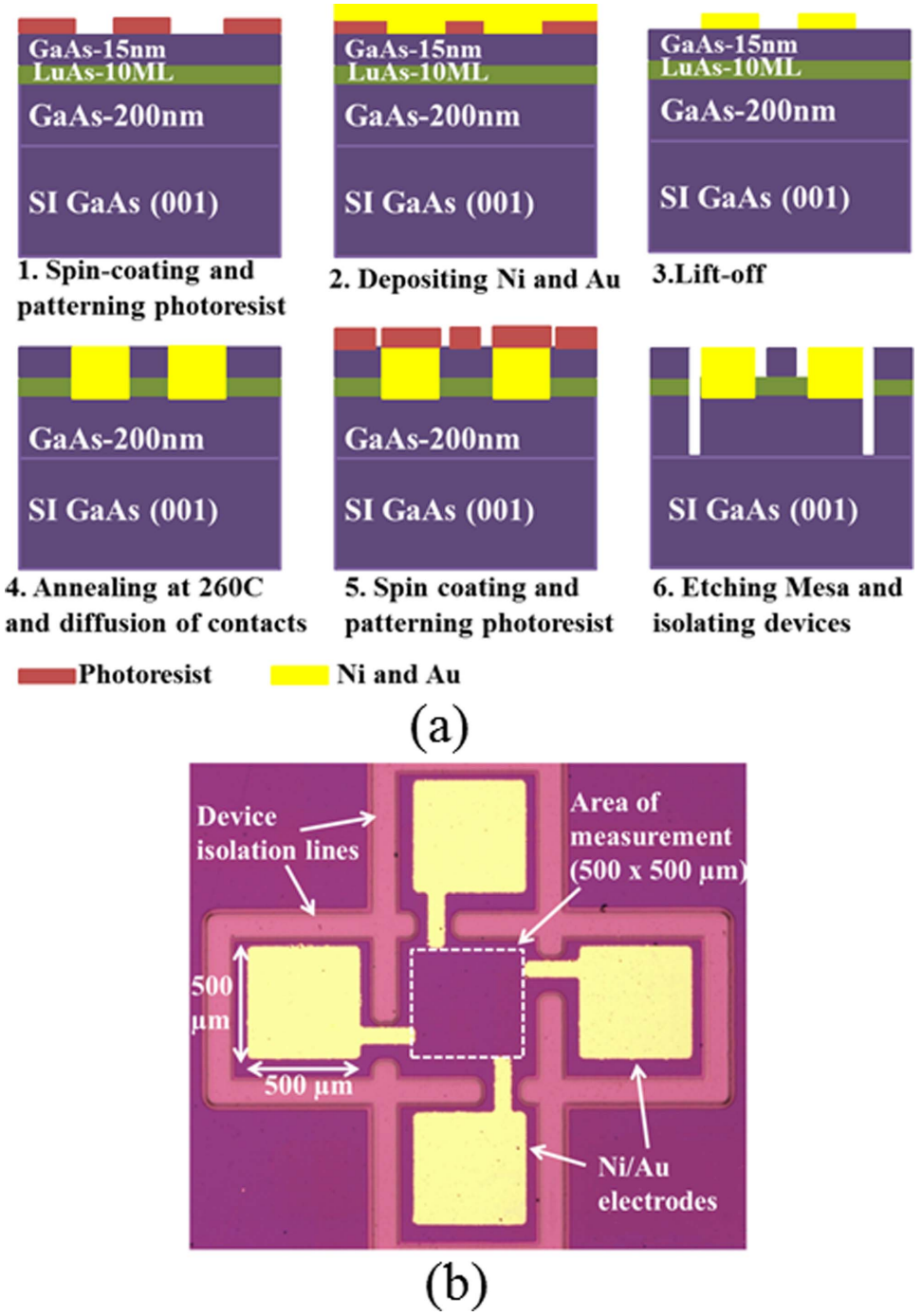

FIG. 1. (a) Illustration of the fabrication process of Van der Pauw (VDP) structures on $La_xLu_{1-x}As$ films on semi-insulating (SI) GaAs substrates. (b) Optical image of the VDP structure fabricated on 10 ML LuAs sample.

where m, e, n and v_d are the mass, charge, density and the drift velocity of carriers in LuAs, respectively, a is the lattice constant of the stoichiometric compound, (lattice constant of the rocksalt phase of LuAs is 5.6751 °A), and x_i is the atomic fraction of the impurity atoms in the lattice. According to (1), increasing the La content from 5 to 9% causes a ∼1.8X increase in ρ_o and from 9 to 15% gives rise to 1.6X increase in ρ_o. While our data shows an increase of ∼1.8X in the resistivity

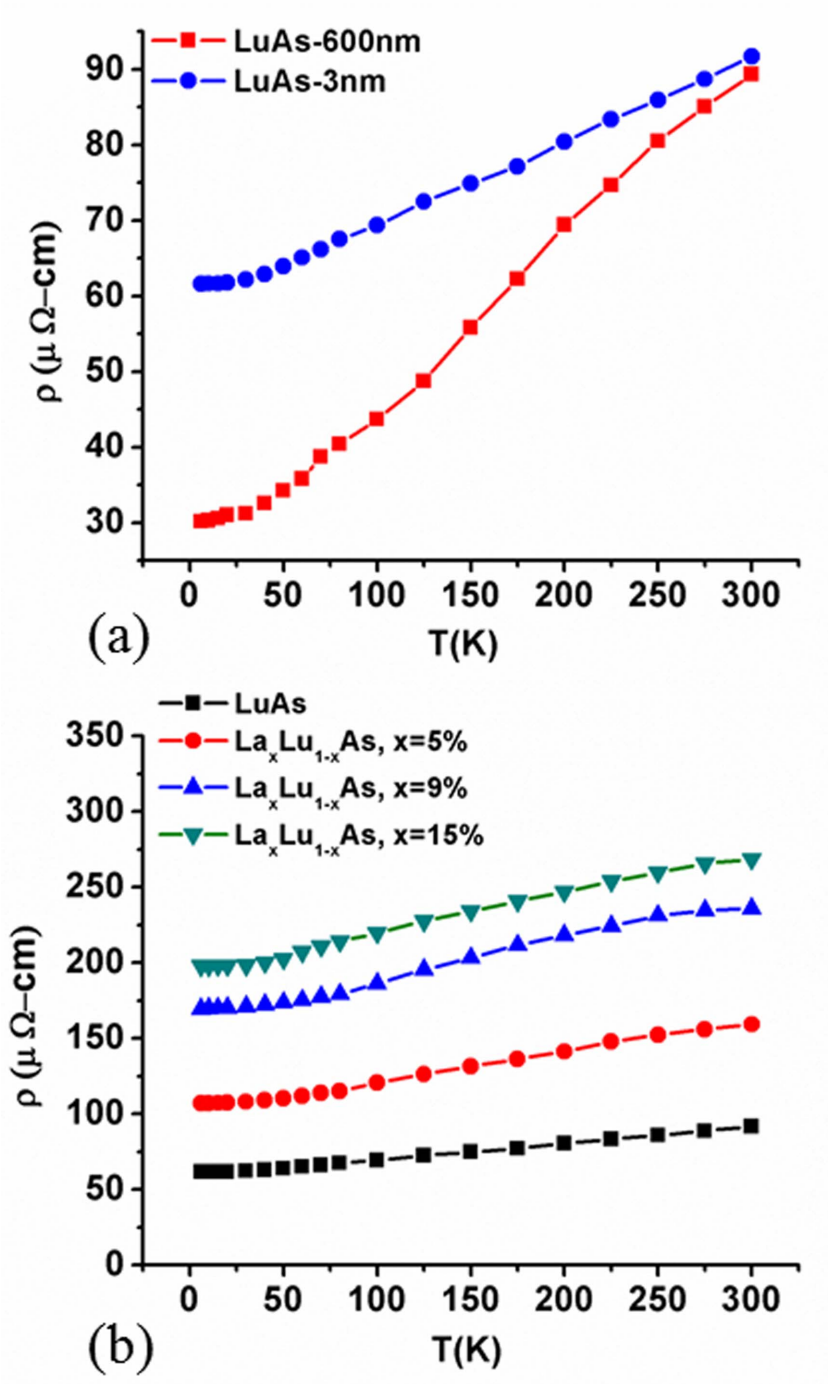

FIG. 2. (a) Temperature-dependent resistivity of thick (600 nm) and thin (10 ML) LuAs films over the 5–300 K range, (b) Temperature-dependent resistivity of $La_xLu_{1-x}As$ films with x = 0, 5, 9 and 15 % La content shows an increase in the resistivity values with increasing La.

of $La_xLu_{1-x}As$ (x = 9%) compared to that of $La_xLu_{1-x}As$ (x = 5%), the increase in the resistivity of $La_xLu_{1-x}As$ (x = 15%) compared to $La_xLu_{1-x}As$ (x = 9%) films is only ~1.2X. This reduction in the resistivity increase (compared to prediction from (1)) is likely a result of carrier contribution from La charge carriers.

At higher temperatures, inelastic scattering increases. Using Matthiessen's rule, we separate the contribution of impurities from the thermally activated scattering mechanisms, ρ_i (T):

$$\rho(T) = \rho_o + \rho_i(T) \tag{2}$$

where $\rho(T)$ is the total electrical resistivity. In stoichiometric semimetallic compounds, the temperature-dependent electrical resistivity, $\rho_i(T)$, can be expressed as the sum of the contribution from carriers and phonons:[20]

$$\rho_i(T) = \frac{1}{ne^2}\left(\frac{1/\tau_{phon.} + 1/\tau_{eh}}{1/m_e + 1/m_h}\right) \tag{3}$$

where τ_{Phon} and τ_{eh} are the relaxation times associated with phonon scattering and carrier scattering respectively, and m_e and m_h are the effective mass of electrons and holes. In the remainder of this article, we discuss the temperature, thickness, and alloy composition dependence of the resistivity.

Figure 3(a) shows the $\rho_i(T)$ term of the resistivity of LuAs films in the logarithmic scale over the 20–300 K range. Two separate regions of the resistivity can be identified: 20–80 K and 80–300 K ranges. The resistivity of 10 ML and 600 nm LuAs films in the 20–80 K range is proportional to $T^{2.70}$ and $T^{1.95}$ respectively. In this range, the temperature dependence of 600 nm LuAs films resembles the T^2-dependence which has been observed for certain transition metals, as well as for semimetallic elements such as arsenic and layered semimetallic compounds such as TiS_2.[20,21] This dependence on temperature is attributed to the impact of carrier-carrier scattering. The resistivity of the 10 ML LuAs film in the 20–80 K range shows slightly stronger temperature dependence. This difference could be due to the additional interfacial roughness scattering affecting the carriers in the thinner film.

The quasi-quadratic temperature dependence of the resistivity in the 20–80 K range is also observed for 10 ML $La_xLu_{1-x}As$ films. Figure 3(b) shows the resistivity of $La_xLu_{1-x}As$ films in the logarithmic scale. The resistivity of $La_xLu_{1-x}As$ films in the 20–80 K range is proportional to $T^{2.70}$, $T^{2.41}$, $T^{1.79}$ and $T^{2.37}$ for x = 0, 5, 9 and 15% La content, respectively. The weaker temperature dependence for x = 5 and 9% La content can be understood to arise from increased impurity scattering by La atoms. For x = 15%, as we discussed before, carrier contribution from La becomes appreciable and might explain the increased temperature dependence, however, further studies are needed to elucidate charge transport for relatively large La content (x ≥ 15%).

At higher temperatures above ~80 K (see Figure 3(a)), the temperature dependence of the epitaxial LuAs films is reduced and the resistivity becomes proportional to $T^{1.23}$ and $T^{1.39}$ for 10 ML and 600 nm films respectively. Over this thermal range, the resistivity is likely governed by the lattice scattering. The lattice contribution to the electrical resistivity can be described by the Bloch-Grüneisen function, which is proportional to $\sim T^5$ at temperatures below $\theta_D/10$ and to $\sim T$ at temperatures above $\theta_D/3$, where θ_D is the Debye temperature.[20,21] The Debye temperature is a measure of distinguishing between high and low-temperature regions of the solids. While high frequency phonons are frozen for $T < \theta_D$, all phonon modes are present at $T > \theta_D$.[22]

Theoretical studies based on the elastic constants predict a Debye temperature of ~309 K for LuAs.[23] Therefore, the lattice contribution to the electrical resistivity below ~300 K is mainly due to acoustic phonons, while the impact of high-frequency or optical phonons on carrier scattering becomes significant mostly at temperatures well above ~300 K.[24] Based on this value for θ_D, the low temperature regime of the Bloch-Grüneisen model, where the resistivity is expected to show T^5 dependence, is within the range where the impact of impurity scattering is non-negligible. The high temperature regime of the lattice scattering begins from approximately 100 K. The Debye temperature is reported to be 301 K for LaAs,[14] which is also estimated based on data of elastic constant. Accordingly, it is expected that the approximately linear temperature dependence of resistivity due to phonon scattering will become observable at temperatures above ~100 K. In our experimental studies, above 80 K, the resistivity of $La_xLu_{1-x}As$ films is proportional to $T^{1.23}$, $T^{1.40}$, $T^{1.43}$ and $T^{1.13}$ for x = 0, 5, 9 and 15% of La content, respectively.

The thicker LaAs and $La_xLu_{1-x}As$ films studied in this work show a similar trend to the thin films. In Table I we present the resistivity of 600 nm LuAs along with those of 500 nm LaAs and $La_{0.48}Lu_{0.52}As$ at 300 K, 80 K and 5 K. The resistivity of 150 nm ErAs is provided for comparison.[25]

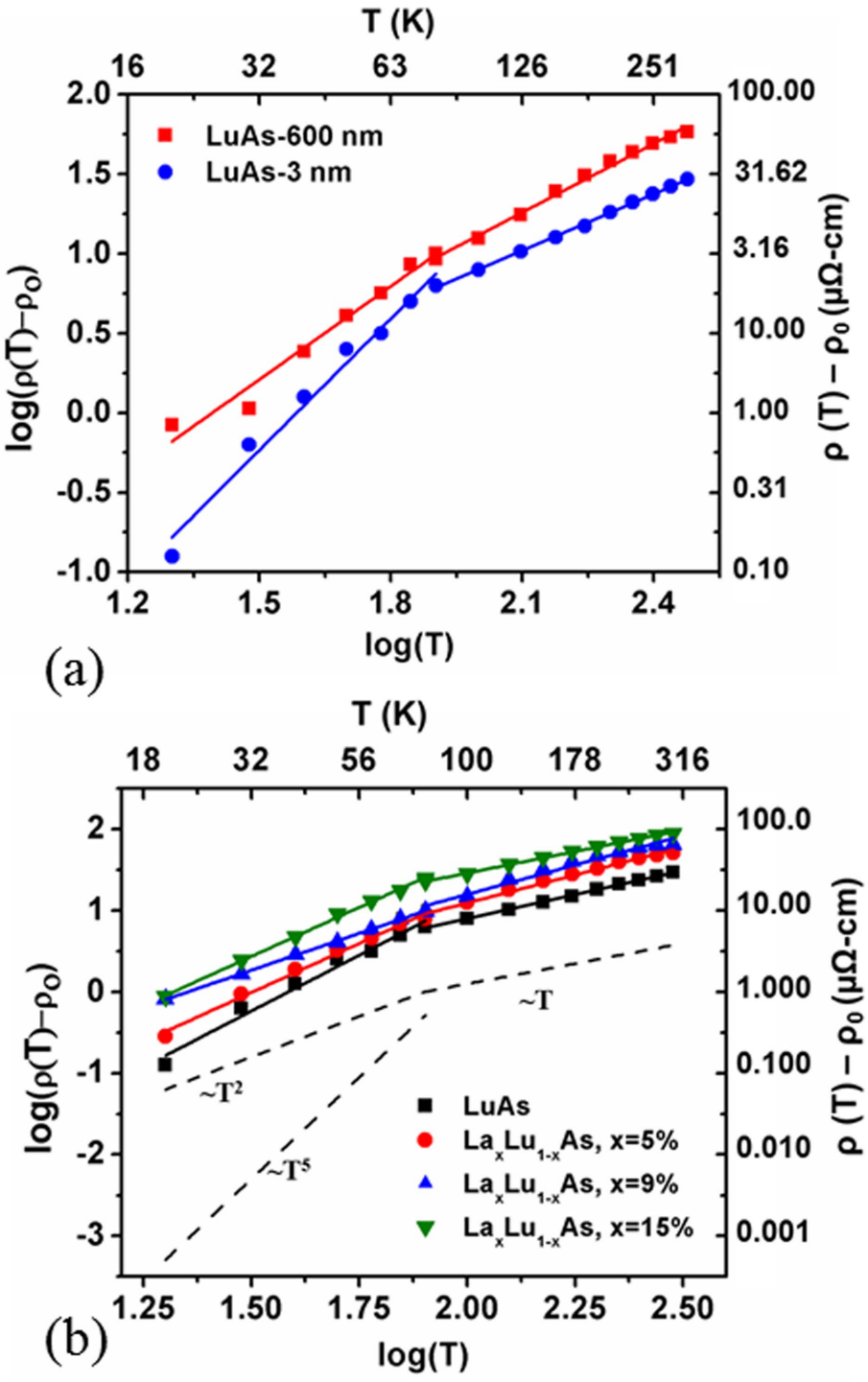

FIG. 3. (a) Resistivity of the thick and thin LuAs films over the 20-300 K range in the logarithmic scale shows two separate regions, below 80 K, where the resistivity is proportional to $T^{2.70}$ and $T^{1.95}$ for 10 ML and 600 nm films, suggesting that carrier-carrier scattering is dominant, and above 80 K where the resistivity is proportional to $T^{1.23}$ and $T^{1.39}$ for 10 ML and 600 nm films indicating that phonon scattering is dominant. (b) Resistivity of $La_xLu_{1-x}As$ alloy films with x = 0, 5, 9 and 15 % over the 20–80 K range in the logarithmic scale can also be separated into two regions. Below 80 K, the resistivity is proportional to T^y where y is in the range of 1.79–2.7 and above 80 K where y is in the range of 1.13–1.43.

TABLE I. Resistivity of 500 nm thick $La_{0.48}Lu_{0.52}As$ and LaAs, and 600 nm thick LuAs at selected temperatures.

Compound	ρ (5 K) [$\mu\Omega$-cm]	ρ (78 K) [$\mu\Omega$-cm]	ρ (300 K) [$\mu\Omega$-cm]
LuAs (600 nm)	30.17	40.43	89.35
LaAs (500 nm)	—	327.72	602.64
$La_{0.48}Lu_{0.52}As$ (500 nm)	120.13	166.03	302.82
ErAs (150 nm)[25]	16.10	22.74	61.41

The resistivity values for the 500 nm $La_xLu_{1-x}As$ (x = 48%) film is between those of the composing binaries at 300 K and 80 K. Moreover, since the θ_D calculated for LaAs (301 K) is close to that of LuAs, one expects to see that the effect of the lattice scattering in the $La_xLu_{1-x}As$ (x = 48%) film becomes significant at the same temperature range as it does for LuAs and LaAs.

Besides the above-mentioned scattering mechanisms, the interfacial roughness is believed to have a substantial impact on the carrier mobility of 10 ML LuAs films. The interfacial scattering becomes significant when the thickness of the film becomes comparable to the mean free path of the carriers.[26,27] To the best knowledge of the authors, the carrier mean free path in LuAs and LaAs has not been reported so far. The reported values for the mean free path of hot carriers for ErAs films with a thickness of 100-300 °A is ∼100 °A at 80 K.[28] Assuming the mean free path of carriers in ErAs can be used as a reasonable rough estimate of the mean free path of carriers in LuAs and LaAs, one can see that the interfacial roughness scattering can have a significant impact on the resistivity of 10 ML (∼3 nm) LuAs film compared to 600 nm films. The roughness scattering is believed to affect the carrier scattering of 10 ML $La_xLu_{1-x}As$ likewise. It becomes relatively weaker compared to thermally activated scattering mechanisms at higher temperatures.[29]

In conclusion, we have experimentally studied the temperature-dependent electrical resistivity of the rare-earth compound $La_xLu_{1-x}As$ and its constituent binaries down to 10 monolayers. We found that the electrical resistivity of $La_xLu_{1-x}As$ and its constituent binaries is consistent with that of semimetallic systems. The resistivity is separated into impurity, carrier and lattice scattering regions. Impurity scattering causes a constant residual resistivity for all samples below 20 K, while carrier scattering is understood to be the dominant scattering mechanism in the 20–80 K range. Above 80 K, phonon scattering becomes the dominant scattering mechanism. Finally, the ability to grow high-quality $La_xLu_{1-x}As$ films on III-V substrates opens up the possibility to develop novel device applications for these rare-earth crystalline materials.

This work was supported by the Army Research Office through YIP award (W911NF-11-1-0455) and the PECASE (W911NF-09-1-0434). Sample fabrication was performed at the Microelectronics Research Center, a member center of the National Science Foundation National Nanotechnology Infrastructure Network.

[1] C. G. Duan, R. F. Sabirianov, W. N. Mei, P. A. Dowben, S. S. Jaswal, and E. Y. Tsymbal, J. Phys.: Condens. Matter **19**, 315220 (2007).
[2] C. J. Palmstrøm, K. C. Garrison, S. Mounier, T. Sands, C. Schwartz, N. Tabatabaie, S. Allen, H. Gilchrist, and P. Miceli, J. of Vac. Sci. Technol. B **7**, 747–752 (1989).
[3] L. H. Brixner, J. Inorg. Nucl. Chem. **15**, 199–201 (1960).
[4] S. J. Allen, N. Tabatabaie, C. J. Palmstrøm, G. W. Hull, T. Sands, F. DeRosa, H. L. Gilchrist, and C. Garrison, Phys. Rev. Lett. **62**, 2309–12 (1989).
[5] A. G. Petukhov, W. R. L. Lambrecht, and B. Segall, Phys. Rev. B **53**, 4324–4339 (1996).
[6] W. R. Lambrecht, Phys. Rev. B **62**, 13538–13545 (2000).
[7] M. Said, F. Ben Zid, C. M. Bertoni, and S. Ossicini, Eur. Phys. J. B **23**, 191–199 (2001).
[8] S. J. Allen, F. DeRosa, C. J. Palmstrøm, and A. Zrenner, Phys. Rev. B **43**, 9599–9609 (1991).
[9] A. G. Petukhove, W. R. L. Lambrecht, and B. Segall, Phys. Rev. B **50**, 7800–04 (1994).
[10] M. P. Hanson, A. C. Gossard, and E. R. Brown, Appl. Phys. Lett. **89**, 111908 (2006).
[11] S. J. Allen, D. Brehmer, and C. J. Palmstrøm, MRS Proceedings **301**, 307 (1993).
[12] D. E. Brehmer, K. Zhang, C. J. Schwarz, S. P. Chau, S. J. Allen, J. P. Ibbetson, J. P. Zhang, C. J. Palmstrøm, and B. Wilkens, Appl. Phys. Lett. **67**, 1268–1270 (1995).
[13] M. P. Hanson, A. C. Gossard, and E. R. Brown, J. Appl. Phys. **102**, 043112 (2007).
[14] E. Deligöz, K. Çolakoğlu, Y. Ö. Çiftçi, and H. Özişik, J. Phys.: Condens. Matter **19**, 436204 (2007).

[15] E. M. Krivoy, S. Rahimi, H. Nair, R. Salas, S. J. Maddox, D. J. Ironside, Y. Jiang, V. D. Dasika, D. A. Ferrer, G. Kelp, G. Shvets, D. Akinwande, and S. R. Bank, Appl. Phys. Lett. **101**, 221908 (2012).
[16] E. M. Krivoy, H. P. Nair, A. M. Crook, S. Rahimi, S. J. Maddox, R. Salas, D. A. Ferrer, V. D. Dasika, D. Akinwanded, and S. R. Bank, Appl. Phys. Lett. **101**, 141910 (2012).
[17] E. M. Krivoy, H. P. Nair, R. Salas, S. J. Maddox, D. J. Ironside, G. Kelp, S. Rahimi, D. Akinwande, M. L. Lee, and S. R. Bank, in preparation (2013).
[18] M. G. Buehler and W. R. Thurber, J. Electrochem. Soc. **125**, 645–650 (1978).
[19] M. Vijaya and G. Rangarajan, *Materials Science* (McGraw Hill, 2004).
[20] C. A. Kukkonen and P. F. Maldague, Phys. Rev. Lett. **37**, 782–785 (1976).
[21] J. Heremans, J. P. Issi, A. A. M. Rashid, and G. A. Saunders, J. Phys. C **10**, 4511–4522 (1977).
[22] Christman J. R., *Fundamentals of Solid State Physics* (Wiley, New York, 1988).
[23] G. Pagare, S. S. Chouhan, P. Soni, S. P. Sanyal and M. Rajagopalan, Comput. Mater. Sci. **50**, 538–544 (2010).
[24] W. Kim, S. L. Singer, A. Majumdar, D. Vashaee, Z. Bian, A. Shakouri, G. Zeng, J. E. Bowers, J. M. O. Zide and A. C. Gossard, Appl. Phys. Lett. **88**, 242107 (2006).
[25] J. D. Ralston, H. Ennen, P. Wennekers, P. Hiesinger, N. Herres, J. Schneider, H. D. Müller, W. Rothemund, F. Fuchs, J. Schmälzlin, and K. Thonke, J. Electron. Mater. **19**, 555–560 (1990).
[26] E. H. Sondheimer, Adv. Phys. **50**, 499–537 (2001).
[27] Y. Hanaoka, K. Hinode, K. Takeda, and D. Kodama, Mater. Trans. **43**, 1621–1623 (2002).
[28] K. J. Russell, V. Narayanamurti, I. Appelbaum, M. P. Hanson, and A. C. Gossard, Phys. Rev. B **74**, 205330–5 (2006).
[29] H. Sakaki, T. Noda, K. Hirakawa, M. Tanaka, and T. Matsusue, Appl. Phys. Lett. **51**, 1934–1936 (1987).